Assessing and Optimizing Free Space Luminescent Solar Concentrators for Urban Façade Installation

Shweta Pal[1] and Rebecca Saive[1]

[1]University of Twente, Overijssel, Enschede, 7522NB, the Netherlands.

2022 IEEE 49th Photovoltaics Specialists Conference (PVSC) | 978-1-7281-6117-4/22/$31.00 ©2022 IEEE | DOI: 10.1109/PVSC48317.2022.9938733

***Abstract*— Net-zero energy buildings (NZEBs) for urban settings require novel building-integrated photovoltaic systems, to enable optimal use of available land. Free-space luminescent solar concentrators (FSLSCs) can concentrate incoming irradiance into a smaller cone, such that, when optimally positioned around a bifacial module, can enhance photovoltaic output. In this work, we assess and optimize an FSLSC façade for enhancing the yield of a bifacial module-based fence. Using a reverse ray-tracing based algorithm, we calculated the short-circuit current density, the total power per unit area and the module current mismatch induced by the FSLSC façade. Our calculations show a relative power per unit area enhancement of ~36% and ~111% by an optimized FSLSC façade, as compared to a white-painted diffuse and an ideal black façade, respectively.**

Keywords—Free-space luminescent solar concentrator, Luminescent solar concentrator, Exotic reflectors, Albedo, Yield modeling, Bifacial solar cells, Building integrated photovoltaics, BIPV, Reverse ray-tracing, Mismatch, Net-zero energy buildings.

I. Introduction

Net-zero energy buildings (NZEB) sustainably generate energy equal to their annual consumption. The booming market demand for NZEBs [1] require innovative building-integrated photovoltaic (BIPV) designs. Novel BIPV configurations are particularly important for urban settings where the energy demand is high, but free land is scarce and instead, building façades constitute the most abundant type of surface. However, irradiance on façades is often not ideal. A lower cost alternative to directly placing solar panels could be to redirect and concentrate light from façades onto standard (bifacial) solar panels placed in the vicinity of the building (see Fig. 1d). The bifacial module can capture light from both faces, *i.e.*, front (from the sun/sky) and rear (from the façade). The incoming irradiance consists of direct (unscattered) and diffuse (scattered) sunlight. Direct irradiance concentration using lenses and mirrors is a well-understood and mature technology [2-5]. But concentration of diffuse light poses an interesting challenge and is particularly important for cloudy countries with high fraction of diffuse irradiance or for façades applications which do not allow for solar tracking. Focusing such diffuse or randomized light requires energy input to decrease the entropy, *i.e.*, bringing order in a disordered system.

A free-space luminescent solar concentrator (FSLSC) [6] provides a clever way to focus direct and diffuse light onto a solar cell. It consists of a nanophotonic-coating and luminophore embedded waveguide surrounded by Lambertian walls (see Fig. 1a.). The luminophores down-convert the high energy photons (i.e., expends energy) to achieve control. The absorbance and emission peak of a luminophore dye is shown in Fig. 1b. The nanophotonic coating is designed such that it is transparent to the photons within the dye's absorbance peak (λ_{ab}) coming from every direction, and to photons within the dye's emission peak (λ_{em}) only in a small escape cone. The high energy photons (λ_{ab}) enter the structure from every angle, then are red-shifted (λ_{em}) by the dye, finally, leaving through the escape cone. Fig. 1c. shows the spectral and angular reflectance of an ideal optimized nanophotonic coating [7] with a $\pm 20°$ wide escape cone for the wavelength range indicated by λ_{es}. Incoming photons lying between 600 nm and 700 nm (λ_{es}) that are incident within the cone are accepted and emitted again in the same cone (shown by blue region). Whereas if they are incident from outside the cone, they are specularly reflected (shown by the yellow region). All other wavelengths are specularly reflected for all the angles (shown by the yellow area). The Lambertian coating reflects all the photons back into the system diffusively, and prevents leakage or trapping of light due to total internal reflection. Strategic orientation of the FSLSC's escape cone towards a bifacial module can improve the photovoltaic yield. For best results, a) the absorbance range (λ_{ab}) and the quantum yield (QY) of the dye must be maximized, b) λ_{es}, λ_{em} and the wavelengths for which the module's spectral response is the highest must overlap. FSLSCs can also help in yield

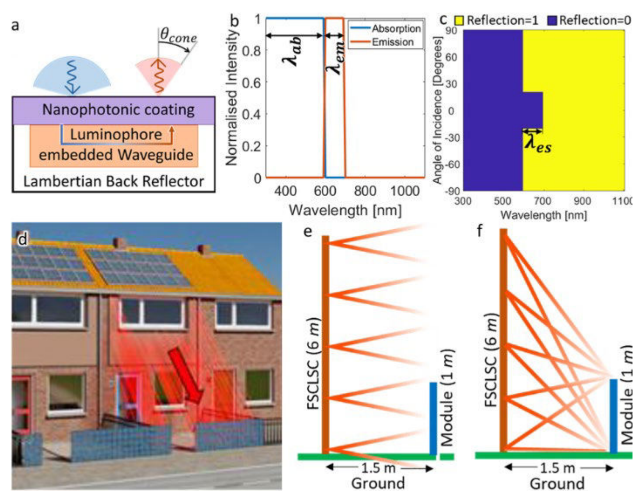

Fig. 1. a) Schematic of a free-space luminescent solar concentrator (FSLSC) with an upright escape cone. b) Spectral absorption and emission profile of an ideal luminophore, c) Spectral and angular reflectance of an ideal nanophotonic coating with a $\pm 20°$ escape cone about 0° with respect to the surface normal. d) Façade integrated FSLSC behind a bifacial module fence. e-f) Schematic of a façade-integrated configuration using unoptimized and optimized façade, respectively.

improvement while keeping the temperature relatively low, as the incoming photons are of lower energy and cannot contribute to heat due to thermalization losses.

FSLSCs can potentially lead to innovative BIPV designs for urban NZEBs. One interesting design involves using an FSLSC as a façade material and positioning a vertical bifacial module in the front as a fence (see Fig. 1d). But a façade fully covered with an FSLSC having fixed, upright cone (see Fig. 1e) will lead to the following issues: 1) the FSLSC points far away from the module will not contribute to power generation as the light from the escape cone will not reach the module, 2) Some FSLSC points will focus light on a passerby or undesirable places like the street or neighboring buildings, 3) FSLSC points near the ground will focus some light on the ground instead of the module. Such a situation leads to wastage of materials and loss of potential yield enhancement. Thus, the cone size and cone tilt of the FSLSC (or nanophotonic coating) must be optimized such that every point on the façade has its cone oriented towards the module only (see Fig. 1f).

For this report, we assess and optimize the performance of an FSLSC façade in front of bifacial module-based fence using a reverse-ray tracing approach. We found a relative power per unit area enhancement of ~36% and ~111% due to an optimized FSLSC facade, as compared to a white-painted diffuse (Reflectance = 0.85[11]) and an ideal black façade, respectively.

II. Output enhanancement by an optimised FSLSC façade

We computationally analyze the output of a bifacial module fence due to an optimized FSLSC façade (as shown in Fig. 1f). We assume the dye properties shown in 1b and a quantum yield of 100%. The absorbed wavelengths were evenly distributed over the emission range (λ_{em}) displayed in Fig. 1b. The short-circuit current density (J_{sc}), total power per unit area (P_{total}) and current mismatch of the module was calculated using a 2D reverse ray-tracing methodology discussed in [8]. The module height was set to be 1 *m*, the house height was set to be 6 *m* (a two-story building), and the separation between them was set to be 1.5 *m* (see Fig. 3a). The module was divided into 100 pixels,

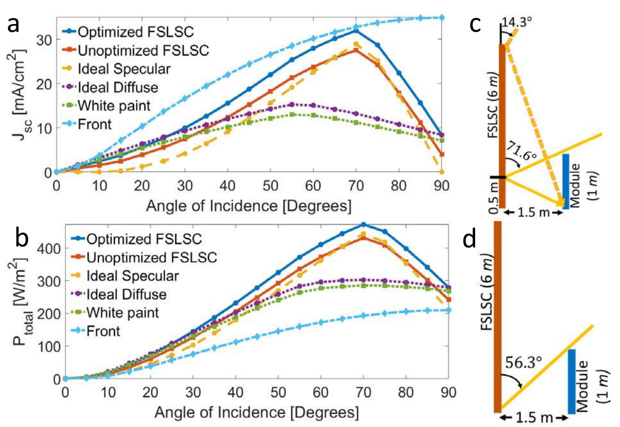

Fig. 2. a) The short-circuit current density (J_{sc}) and b) the total power per unit (P_{total}) of a bifacial module fence due to an optimised FSLSC façade as a function of changing angle of incidence (AoI). c) Schematic showing the minimum AoI for which the specular reflection reaches the module (dashed line) and the minimum AoI which causes shading for a specular façade (solid line). d) Schematic showing the minimum AoI which which causes shading for a diffuse façade.

where module pixel = 1 is the closest to the ground. Similarly, the FSLSC was divided into 600 pixels. AM1.5G [9] was used as the input irradiance and the angle of incidence (AoI) was varied from 0° (vertical relative to the ground) to 90° (horizontal relative to the ground), *i.e.*, solar noon to sunrise or sunset. The incoming irradiance is assumed to consist of parallel rays. For the module, we used a silicon heterojunction bifacial module[10] with bifaciality = 98.8%.

We begin the discussion by evaluating the short-circuit current density (J_{sc}) due to an optimized FSLSC façade. Fig. 2a shows the J_{sc} of the bifacial module fence due to the front illumination (the sun/sky) and the rear illumination (the façade), as a function of the changing angle of the sun. The rear J_{sc} due to an ideal diffuse façade (Reflectance= 1), white-painted façade (Reflectance = 0.85), ideal specular and an unoptimized FSLSC (material properties shown in Fig. 1b and 1c) are also shown for comparison.

At $AoI = 0°$, the irradiance is vertically incident on the ground. Hence, the rays pass tangentially, without interacting with the module and the façade, which leads to zero output. Now, as the sun goes away from the solar noon, the front J_{sc} increases, reaching a maxima at $AoI = 90°$. This is because, at $AoI = 90°$, the sun rays are normally incident on the front face of the cell, thus leading to a maximum output. For a specular reflector, the output becomes non-zero for $AoI \geq 15°$, because specularly reflected rays reach the module only for $AoI > 14.3°$ (see Fig 1c- dashed line). For an unoptimized FSLSC façade, the down-converted photons from 20° cone reach the module which leads to non-zero output. This is only contributed by façade pixels below 1.55 m. An optimized FSLSC façade also contributes down-converted photons but from every pixel due to cone size and tilt optimization. For $AoI > 14.3°$, specular reflection due to unoptimized and optimized FSLSC façade start to contribute as well, thus leading to an increase in output. The rear J_{sc} due to a specular, unoptimized, and optimized FSLSC façade reach a maximum at $AoI = 70°$, since beyond that, shading due to module sets in (see Fig. 2c- solid line). The shading increases with the increasing AoI, which leads to a decline in output. For diffuse reflectors, ideal and white-paint, the output increases as the AoI increases reaching a maximum at $AoI = 55°$. This because shading sets in at $AoI \geq 56.3°$ (see Fig. 2d).

To completely evaluate the feasibility of a configuration, one must calculate the total power output. For this, the front and rear J_{sc} are added to obtain total J_{sc}, which is used to calculate the total power per unit area of the system. The resulting power per unit area for various façade-integrated configurations are plotted in Fig. 2b, and the relative enhancement, i.e., the ratio of area under the curve, was calculated. We observe a relative yield improvement of ~36% due to an optimized FSLSC facade as opposed to a white-painted diffuse façade. On comparison with an ideal black façade (or only front illumination), an optimized FSLSC results in a relative enhancement of ~111%.

III. Mismatch due to an optimized FSLSC façade

To rigorously discuss the merit of a concentrator, one must also calculate the current mismatch introduced on the module by it. Current mismatch is the spatially varying current generation in the module due to spatially varying illumination incident on it. A module, generally, consists of many solar cells connected in series. Therefore, the cells must obey the current matching condition, *i.e.*, every cell must produce the same current. Thus, all the cells drop their current values to match the minimum value. The excess is lost as heat and if this heat is excessive, it can damage the cells. As an FSLSC has a spectrum and angle-dependent reflectance, it can redirect light inhomogeneously onto the module, causing mismatch. The spatially varying short-circuit current density generation along the length of the module due to an optimized FSLSC façade is shown in Fig. 3d.

Before we begin the discussion, it is to be noted that there are two cosine terms associated with every reflected photon (see Fig. 3a and 3b). Namely, 1) cos (θ_R) where θ_R is the angle of reflection relative to the façade's normal, 2) cos (θ_M) where θ_M is the angle at which the module receives the photon relative to its own surface normal. Here, since the façade and the module are parallel to each other, θ_R and θ_M are equal. Also, along the surface normal, the module has the highest external quantum efficiency (EQE), which is the efficiency of absorbed photon to electron conversion at a given wavelength. The EQE eventually reaches zero as the incoming photon angle approaches the surface tangent.

In Fig. 3d, for $AoI = 0°$, the light passes tangentially and does not get redirected to the module. Hence, every pixel on the module generates zero output, causing no mismatch. For $AoI > 0°$, the incoming irradiance starts getting redirected to the module by the façade. Module pixel=100 always generates the highest output at a given AoI. This is because: 1) the illuminated façade pixels emit and reflect at angles for which the $\cos(\theta_R)$ is higher (see Fig. 3a), 2) the module receives the redirected irradiance at a better angle, i.e., higher cos (θ_M) (see Fig. 3a), 3) The EQE is better for those θ_M values. The contribution of these three factors reduces as one moves down along the module (see Fig. 3b), thus leading to a spatially varying short-circuit current density. For $AoI > 70°$, shading of the façade by the module sets in. Because of this, there are no specularly reflected rays reaching near the bottom of the module, thus causing 'self-shading'. The self-shading increases as the AoI increases. For $AoI = 90°$, the mismatch is quite low (range~0.09 mA/cm^2). This is because the specular reflection contribution is zero as either the rays are reflected back in the same direction or there is shading (see Fig. 3c). The mismatch is only due to down-converted photons.

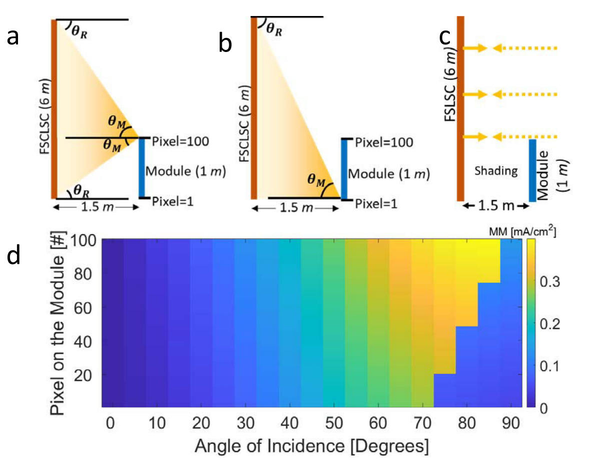

Fig. 3. a-c) Schematic showing the configuration and the angles. d) The spatially varying short-circuit current denisty along the length of a bifacial module fence, as a function of changing angle of incidence, due to an optimised FSLSC façade.

Quantifying the increase in power output and the mismatch can help in assessing the performance and economic feasibility of an FSLSC façade, and further optimize the configuration for desired output. Optimization algorithms can be implemented to improve the final total output or the mismatch introduced by the FSLSC, depending upon the application.

IV. Conclusion

In this report, we computationally assessed and optimized the performance of an FSLSC as a façade for a bifacial module-based fence. We showed that, when optimized, such a façade can lead to a relative output enhancement of ~36% as compared to a white-painted façade (Reflectance=0.85) and ~111% as compared to an ideal black façade. Optimizing the cone size and cone tilt can boost the implementation of FSLSCs as façade materials. Knowledge of the cone size and tilt can also serve as motivation to innovate better nanophotonic coatings, or FSLSC configurations (flexible or tilted FSLSCs). Another improvement can involve maximizing the range of λ_{ab} and quantum yield of the dye, i.e., down-converting more photons for higher output. This can be achieved by using a better dye or using multiple dyes. Our approach enables rigorous assessment and optimizations of FSLSC façade for urban NZEBs, thus bridging the gap between the lab-level devices and their real world applications.

References

[1] Global Industry Analysts, "Global Net-Zero Energy Buildings (NZEBs) Industry Market Report," Global Industry Analysts, July 2021.

[2] M. Abdelhamid, B. K. Widyolar, L. Jiang, R. Winston, E. Yablonovitch, G. Scranton, D. Cygan, H. Abbasi and A. Kozlov, "Novel double-stage high-concentrated solar hybrid photovoltaic/thermal (PV/T) collector with nonimaging optics and GaAs solar cells reflector," *Applied Energy,* vol. 182, pp. 68-79, November 2016.

[3] K.K. Chong, S.L. Lau, T.K. Yew and P. C.L. Tan, "Design and development in optics of concentrator photovoltaic system," *Renewable and Sustainable Energy Reviews,* vol. 19, pp. 598-612, March 2013.

[4] Chung-Yu Tsai, "Improved irradiance distribution on high concentration solar cell using free-form concentrator," *Solar Energy,* vol. 115, pp. 694-707, May 2015.

[5] Z. Zhuang and F. Yu, "Optimization design of hybrid Fresnel-based concentrator for generating uniformity irradiance with the broad solar spectrum," *Optics & Laser Technology,* vol. 60, pp. 27-33, August 2014.

[6] L. Einhaus and R. Saive, "Free-Space Concentration of Diffused Light for Photovoltaics," in *47th IEEE PVSC*, 2020.

[7] G. Heres, L. Einhaus and R. Saive, "Analytical Model for the Performance of a Free-Space Luminescent Solar Concentrator," in *IEEE Photovoltaic Specialists Conference (PVSC)*, online, 2021.

[8] S. Pal and R. Saive, "Investigating Bifacial Photovoltaic Output Under Diffuse, Specular and Glossy Albedo," in *OSA PVLED - Optical Devices and Materials for Solar Energy and Solid-state Lighting*, Online, July 2021.

[9] "E891-87 American Society for Testing and Materials, Annual Book of ASTM Standards," Standard Tables for Terrestrial Direct Normal Solar Spectral Irradiance for Air Mass 1.5.

[10] S. Pal, A. Reinders and R. Saive, "Simulation of Bifacial and Monofacial Silicon Solar Cell Short-Circuit Current Density Under Measured Spectro-Angular Solar Irradiance," *IEEE Journal of Photovoltaics,* vol. 10, no. 6, pp. 1803-1815, 2020.

[11] S. Sharples and S. Mahambrey, "Reflectance distributions and atrium daylight levels: a model study," *International Journal of Lighting Research and Technology,* vol. 31, no. 4, pp. 165-170, 1999.